Synthesis of Mesoporous Carbons with Controllable N-Content and Their Supercapacitor Properties†

Jeongnam Kim, Minkee Choi, and Ryong Ryoo*

National Creative Research Initiative Center for Functional Nanomaterials, Department of Chemistry (School of Molecular Science BK21), Korea Advanced Institute of Science and Technology, Daejeon 305-701, Korea
**E-mail: rryoo@kaist.ac.kr*
Received July 25, 2007

A synthesis route to ordered mesoporous carbons with controllable nitrogen content has been developed for high-performance EDLC electrodes. Nitrogen-doped ordered mesoporous carbons (denoted as NMC) were prepared by carbonizing a mixture of two different carbon sources within the mesoporous silica designated by KIT-6. Furfuryl alcohol was used as a primary carbon precursor, and melamine as a nitrogen dopant. This synthesis procedure gave cubic *Ia*3*d* mesoporous carbons containing nitrogen as much as 13%. The carbon exhibited a narrow pore size distribution centered at 3-4 nm with large pore volume (0.6-1 $cm^3 g^{-1}$) and high specific BET surface area (700-1000 $m^2 g^{-1}$). Electrochemical behaviors of the NMC samples with various N-contents were investigated by a two-electrode measurement system at aqueous solutions. At low current density, the NMC exhibited markedly increasing capacitance due to the increase in the nitrogen content. This result could be attributed to the enhanced surface affinity between carbon electrode and electrolyte ions due to the hydrophilic nitrogen functional groups. At high current density conditions, the NMC samples exhibited decreasing specific capacitance against the increase in the nitrogen content. The loss of the capacitance with the N-content may be explained by high electric resistance which causes a significant IR drop at high current densities. The present results indicate that the optimal nitrogen content is required for achieving high power and high energy density simultaneously.

Key Words : Nitrogen doping, Mesoporous carbon, EDLC

Introduction

Electric double layer capacitors (EDLCs), also referred to as supercapacitors, have attracted much attention as an electrical energy storage system.[1] The main advantage of the EDLC devices is their ability to generate high specific powers exceeding 10 kW kg^{-1}. The rapid discharge ability makes EDLC suitable as an electrical power component for hybrid cars, digital telecommunication systems, and UPS (uninterruptible power supply) for computers.[2,3] EDLCs are bridging the gap between conventional electrolytic capacitors and batteries, due to the high energy density and high power density. EDLCs also show superior rate capability and long cycle life (over 10^6 cycles) compared with modern secondary batteries.

The high capacitance of EDLC is produced by the quick formation of electrical double layer at electrode/electrolyte interface, which accumulates electrical charges on the electrode surface. On the basis of the mechanism, porous electrode materials with high surface area, capable of high charge accumulation, are demanding for high capacitance.[4] With this regard, activated carbons with high surface area have been most widely used as an EDLC electrode. The sole presence of small micropores (< 2 nm) in the activated carbons, however, often limited the performances of EDLCs due to the limited accessibility and slow molecular diffusion of electrolytes.[5,6]

Recently, ordered mesoporous carbons having enlarged pore diameters have been synthesized by using mesoporous silica as a template.[7] Due to their high surface area (500-2500 $m^2 g^{-1}$), large pore diameter (3-5 nm) and 3-dimensional pore connectivity, mesoporous carbons attracted much attention as an advanced EDLC electrode. The carbon materials showed remarkably enhanced electrolyte transport and exhibited much higher EDLC performances at high current density conditions.[8-11] The well defined and tunable mesoporous structure provided an ideal model electrode system for analyzing the correlation between the EDLC capacitance and carbon pore structure.

In the present work, we demonstrate a synthesis route to the ordered mesoporous carbons with controllable nitrogen content and their electrochemical properties in EDLC applications. It has been pointed out that the doping of heteroatoms such as nitrogen and oxygen in the carbon framework can also markedly increase the EDLC capacitance.[12-17] The presence of heteroatoms was proposed to make the carbon surface more polar and increase the surface affinity to aqueous electrolytes. Furthermore, pseudocapacitance seemed to be generated at such heteroatoms.[4,5,13,14] In this regard, the development of mesoporous carbons containing heteroatom was expected to be highly important for the design of high-performance EDLC electrode materials. Xia *et al.*[18] synthesized N-doped mesoporous carbons with

†This paper is dedicated to Professor Sang Chul Shim on the occasion of his honorable retirement.

graphitic framework by using a CVD method. Lu *et al.*[19] carbonized polyacrylonitrile (PAN) for the synthesis of N-containing mesoporous carbons. However, none of the synthesis strategies allowed the systematic control of nitrogen content in mesoporous carbon frameworks. On this ground, our synthesis route to carbons with well-defined mesopores and controllable nitrogen content would provide an opportunity for more systematic examination of the correlation between heteroatom content and electrochemical properties.

Experimental

Materials. The mesoporous carbons with variable N-content were synthesized by carbonizing a mixture of two different carbon precursors: furfuryl alcohol as a primary carbon precursor and melamine as a nitrogen dopant, respectively. Four samples with different N-content were prepared and denoted as NMC-n, where n is the nitrogen content (wt %) of the resultant materials. In a typical synthesis batch, 0.83 g furfuryl alcohol was infiltrated into 1 g of KIT-6 mesoporous silica incorporating Al (Si/Al = 40).[20] The Al incorporated at the silica mesopore wall served as an acid catalyst for polymerization of furfuryl alcohol. The sample was heated at 373 K for 1 h, and further heated at 623 K for 3 h for the partial carbonization. After cooled to room temperature, the sample was infiltrated with an additional amount of furfuryl alcohol. Then, the sample was physically mixed with melamine. For 1 g of KIT-6, the additional amounts of furfuryl alcohol and melamine were varied in four different sets (g/g): (0.59/0), (0.58/0.08), (0.53/0.75), (0.34/3.0). The mole percentage of furfuryl alcohol/melamine in each set was as follows: (100/0), (90/10), (48/52), (13/87). The mixtures were transferred to the laboratory-made quartz reactor equipped with a porous plug for the carbonization at 1173 K under self-generated, non-combustive gas atmosphere. The resultant carbon/silica composite was washed with HF solution (10% in water/ethanol mixture) to remove the silica template. The resultant carbon samples were referred to as NMC-n with n = 0, 2, 8, 13 according to their nitrogen content, respectively.

Characterizations. Nitrogen content was determined by using an elemental analyzer (Eager300, ThermoFinnigan). Synchrotron powder X-ray diffraction (XRD) patterns were collected using BL8C2 at Pohang Light Source in the reflection mode (λ = 0.154250 nm). Nitrogen adsorption-desorption isotherms were obtained with a Quantachrome Autosorp-1MP instrument at 77 K. All samples were out-gassed under vacuum for 6 h at 573 K before the measurement. X-ray photoelectron spectroscopy (XPS) studies were carried out using VG ESCA2000 with an Mg Kα source, and the C1s peak at 284.6 eV was taken as an internal standard.

Electrochemical measurements. The specific capacitance was performed in a two-electrode cell operating in the galvanostatic charge/discharge mode (WBCS3000 battery cycler, Won A Tech).[6] Two film electrodes (area = 0.78 cm^2) were separated by a porous polypropylene sheet (Celgard), and sandwiched between platinum current collectors. Aqueous solution of 2 M H_2SO_4 was used as the electrolyte solution. For electrode preparation, the mesoporous carbon sample was mixed with polyvinylidene fluoride binder (purchased from Aldrich) and carbon black (CB, Vulcan XC-72 from Cabot). The ratio of sample:binder:CB was 80:10:10 in weight %. The mixture was then pelletized by pressing with a cylindrical steel molder under 1000 psi. The resultant electrode films were evacuated at 393 K for 4 h. The mass of the electrodes varied in the range of 18-20 mg. Before the measurement of capacitance, the electrolyte solution containing the two-electrode cell was treated under vacuum conditions at room temperature for 3 h, in order to remove the residual air remaining in the electrode. Subsequently, the EDLC cell was cycled with 40 times of charge-discharge at a constant current 10 mA cm^{-2}. The cell was charged to 0.9 V with a constant current 10 mA cm^{-2}, charged at a constant voltage of 0.9 V for 30 min, and discharged at a current density of 1-50 mA cm^{-2}. The specific capacitance was then calculated by $I\Delta t/\Delta V$, where I is the constant discharging current, Δt is the discharging time, ΔV is the voltage change. To avoid the effect of the initial voltage drop (IR drop, originated from the internal resistance), the capacitance calculation was carried out in the voltage drop range from 0.35 to 0.45 V in the linear region of V-t curve. The electric conductivity of the carbon electrodes was measured by the four-probe method on pellet that was compacted under the same pressure (1.4 MPa) as the cylindrical pellets.[21] The energy (W) was calculated as $W = 0.5CV^2$, where C is the capacitance and V is the initial voltage after subtracting IR drop. The power (P) was calculated as $P = W/\Delta t$, where W is the energy and Δt is the time spent in the discharge.

Results and Discussion

All NMC carbons exhibited the well-resolved (211) and (220) peaks in the low angle region (Figure 1a), which can be assigned to the diffractions of the cubic *Ia*3*d* space group. The XRD patterns, showing higher order diffraction peaks,

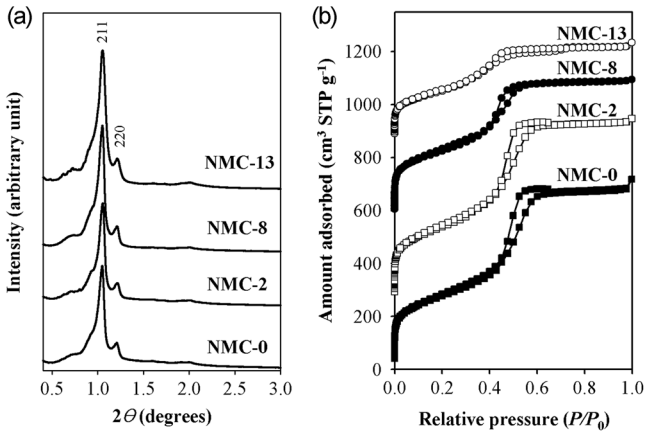

Figure 1. (a) Synchrotron powder X-ray diffraction patterns and (b) N_2 adsorption isotherms for N-doped mesoporous carbons. The isotherms for NMC-2, 8 and 13 samples were offset vertically by 250, 550 and 850 cm^3 STP g^{-1}, respectively.

Table 1. Textural properties of N-doped mesoporous carbons

Sample	S_{BET} [a] ($m^2 g^{-1}$)	W_{BJH} [b] (nm)	V_{total} [c] ($cm^3 g^{-1}$)	V_{micro} [d] ($cm^3 g^{-1}$)	V_{meso} [d] ($cm^3 g^{-1}$)
NMC-0	947	4.1	1.04	0.08	0.96
NMC-2	994	4.0	1.05	0.07	0.98
NMC-8	932	3.9	0.82	0.10	0.72
NMC-13	725	3.1	0.57	0.02	0.55

[a]S_{BET} is the apparent BET specific surface area. [b]W_{BJH} is a mesopore diameter calculated using the BJH method. [c]V_{total} is the pore volume at relative pressure 0.95. [d]V_{micro} is the micro pore volume determined by t-plot method and V_{meso} is the mesopore volume that is equal to $V_{total}-V_{micro}$.

are the indication of the long range ordering, similar to the case of KIT-6 silica template. This result indicates that the highly ordered mesoporous structure is retained regardless of N-doping into the carbon framework. The N_2 adsorption isotherms (Figure 1b) reveal that all NMC carbons are highly mesoporous with narrow pore-size distribution, centered at 3-4 nm. The pore structure properties of NMCs are summarized in Table 1.

XPS was used for analyzing the chemical nature of nitrogen atoms within the carbon framework. The complex XPS N1s spectra of N-doped carbons were fitted to four components of binding energies at 398.7, 400.4, 401.4 and 403 eV (Figure 2 and Table 2).[13] These peaks can be assigned to different forms of nitrogen atoms substituted for carbon in graphene layer: N-6, N-5, N-Q and N-X, respectively.[13] N-6 is pyridinic-N, *i.e.*, nitrogen bonded to two carbon atoms at the edge of graphene layer. N-5 represents pyrrolic-N in five membered ring and/or pyridonic-N. The latter is pyridinic-N which is adjacent to phenolic or carbonyl groups. N-Q corresponds to quaternary nitrogen that is bonded to three carbon atoms in central region of graphene layers. Finally, N-X is pyridine N-oxide. The results showed that the distribution of nitrogen chemical states is significantly depending on the degree of nitrogen doping. It is noteworthy that regardless of nitrogen content the majority of nitrogen atoms are located at the edges of graphene layers (N-6 + N-5 + N-X) while nitrogen atoms located at the central region of graphene layers (*i.e.*, N-Q) contribute to a minor portion.

For the investigation of electrochemical properties of carbon materials, the EDLC capacitances of the mesoporous carbons were measured by a galvanostatic charge/discharge method using two-electrode system. In Figure 3a, the specific capacitances of NMC samples were given as a function of the discharge current density. At low current density, the EDLC capacitances markedly increased with N-content. As noted by Frackowiak and co-workers,[13] the positive effect of nitrogen seems to be twofold. Firstly, the presence of the

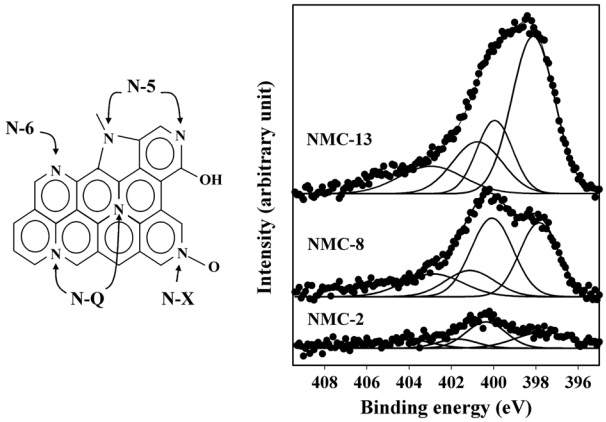

Figure 2. Schematic representation of the nitrogen functional groups in carbon graphene structure (left) and XPS N1s spectra of N-doped mesoporous carbons (right).

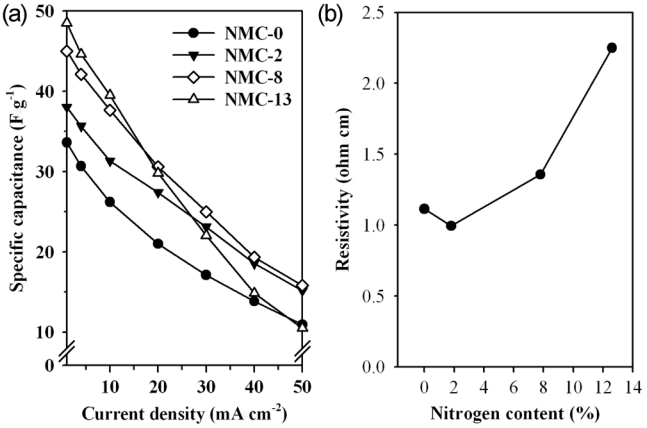

Figure 3. (a) Specific capacitance per unit weight as a function of the discharge current density and (b) electric resistivities of N-doped mesoporous carbons.

polar nitrogen atoms can improve carbon surface affinity to aqueous electrolytes, increasing the truly accessible carbon surface area for the electrolytes. Recently, Kyotani *et al.*[22] performed water vapor adsorption experiment with N-containing carbons and showed that N-containing carbon have superior affinity to the water molecule than pure carbons. Secondly, the pseudocapacitance may be generated at the nitrogen functional groups (possibly due to the oxidation/reduction reaction of pyridinic ring), leading to a large increase in EDLC capacitances. Since most of the nitrogen atoms are located on the periphery of graphene layers (as indicated by XPS), both effects would be more significant.

At high current density conditions (> 30 mA cm^{-2}), the mesoporous carbons with low nitrogen content (NMC-2 and

Table 2. Distribution of nitrogen species in NMC carbons

Sample	N/(C+N) (%)	XPS analysis				
		N-6 (%) 398.7 ± 0.2 eV	N-5 (%) 400.4 ± 0.2 eV	N-Q (%) 401.4 ± 0.2 eV	N-X (%) 403 ±0.2 eV	N-6 + N-5 + N-X (%)
NMC-2	1.8	33.1	38.8	13.5	14.6	86.5
NMC-8	7.8	32.6	37.4	14.5	15.5	85.5
NMC-13	12.6	49.2	19.1	18.8	12.9	81.2

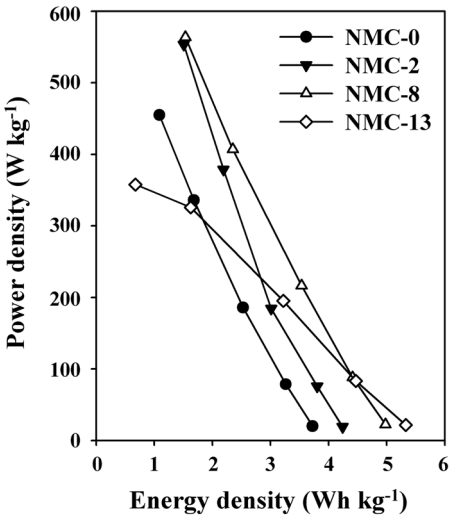

Figure 4. Ragone plots for N-doped mesoporous carbons with various N-contents.

NMC-8) exhibited large specific capacitances. Among the samples with different nitrogen content, the mesoporous carbon with high N-content (NMC-13) showed the fastest drop of capacitance against the increasing current density. Such fast drop of the capacitance can be ascribed to the high electric resistivity of highly N-doped carbon, which causes a significant IR drop at high current density conditions (Figure 3b). It was confirmed that the electric resistivity was lowest at low N-doping (NMC-2) and increased significantly with the further increase of N-doping. Derradji *et al*.[23] reported a similar result and proposed that the small amount of nitrogen might act as an impurity center in graphitic structures which increased the electric conductivity. At high N-doping, however, formation of numerous pyridine-like structures and nitrile bonds might interrupt the interconnections of the graphitic structures, increasing the electric resistivity.

The electrochemical properties of NMC carbons are summarized in a Ragone plot (Figure 4), which clearly demonstrates the energy and power density of the carbon materials. The mesoporous carbons with low N-content (NMC-2 and NMC-8) exhibited both high power density and high energy density compared to the mesoporous carbon without nitrogen doping (NMC-0). In contrast, the energy density of highly N-doped carbon (NMC-13) decreases significantly with increasing power density, due to the large equivalent series resistance (ESR) of two-electrode capacitors.[24,25] These results indicate that the mesoporous carbon with moderate nitrogen contents is the most suitable material for the fabrication of high-performance EDLC electrode.

Conclusion

A synthesis route to the ordered mesoporous carbons with controllable N-content has been developed using two different carbon precursors, *i.e*., furfuryl alcohol as primary carbon precursor and melamine as a nitrogen dopant, respectively. This synthesis strategy allows a facile control of nitrogen content up to 13% in the carbon framework, while the well-ordered mesoporous structures are maintained. The investigation of the EDLC performances with N-doped mesoporous carbons showed that the mesoporous carbons with high N-doping exhibited highest capacitance at low discharge current density, while the carbons with low N-doping exhibited superior capacitance at high current density. The present results indicate that the mesoporous carbons with intermediate N-doping content are most desirable for obtaining both high energy and power density.

Acknowledgment. This work was supported by the Ministry of Science and Technology through Creative Research Initiative Program, and by School of Molecular Science through Brain Korea 21Project. Synchrotron radiation XRD was supported by Pohang Light Source.

References

1. Conway, B. E. *Electrochemical Supercapacitors: Scientific Fundamentals and Technological Applications*; Kluwer-Plenum Press: New York, 1999.
2. Arico, A. S.; Bruce, P.; Tarascon, J. M.; Van-Schalkwijk, W. *Nature Mater.* **2005**, *4*, 366.
3. Kötz, R.; Carlen, M. *Electrochimica Acta* **2000**, *45*, 2483.
4. Frackowiak, E.; Beguin, F. *Carbon* **2001**, *39*, 937.
5. Frackowiak, E. *Phys. Chem. Chem. Phys.* **2007**, *9*, 1774.
6. Endo, M.; Takeda, T.; Kim, Y. J.; Koshiba, K.; Ishii, K. *Carbon Science* **2001**, *1*, 117.
7. Ryoo, R.; Joo, S. H. *Stud. Surf. Sci. Catal.* **2004**, *148*, 241.
8. Yoon, S.; Lee, J. W.; Hyeon, T.; Oh, S. M. *J. Electrochem. Soc.* **2000**, *147*, 2507.
9. Vix-Guterl, C.; Saadallah, S.; Jurewicz, K.; Frackowiak, E.; Reda, M.; Parmentier, J.; Patarin, J.; Beguin, F. *Materials Science and Engineering B* **2004**, *108*, 148.
10. Alvarez, S.; Blanco-Lopez, M. C.; Miranda-Ordieres, A. J.; Fuertes, A. B.; Centeno, T. A. *Carbon* **2005**, *43*, 855.
11. Xing, W.; Qiao, S. Z.; Ding, R. G.; Li, F.; Lu, G. Q.; Yan, Z. F.; Cheng, H. M. *Carbon* **2006**, *44*, 216.
12. Jurewicz, K.; Babel, K.; Ziolkowski, A.; Wachowska, H. *J. Phys. Chem. Solids* **2004**, *65*, 269.
13. Lota, G.; Grzyb, B.; Machnikowska, H.; Machnikowski, J.; Frackowiak, E. *Chem. Phys. Lett.* **2005**, *404*, 53.
14. Hulicova, D.; Kodama, M.; Hatori, H. *Chem. Mater.* **2006**, *18*, 2318.
15. Beguin, F.; Szostak, K.; Lota, G.; Frackowiak, E. *Adv. Mater.* **2005**, *17*, 2380.
16. Frackowiak, E.; Lota, G.; Machnikowski, J.; Vix-Guterl, C.; Beguin, F. *Electrochimica Acta* **2006**, *51*, 2209.
17. Li, W.; Chen, D.; Li, Z.; Shi, Y.; Wan, Y.; Huang, J.; Yang, J.; Zhao, D.; Jiang, Z. *Electrochem. Commun.* **2007**, *9*, 569.
18. Xia, Y.; Mokaya, R. *Adv. Mater.* **2004**, *16*, 1553.
19. Lu, A. H.; Kiefer, A.; Schmidt, W.; Schüth, F. *Chem. Mater.* **2004**, *16*, 100.
20. Gierszal, K. P.; Kim, T.-W.; Ryoo, R.; Jaroniec, M. *J. Phys. Chem. B* **2005**, *109*, 23263.
21. Smits, F. M. *Bell System Tech. J.* **1958**, 711.
22. Hou, P. X.; Orikasa, H.; Yamazaki, T.; Matsuoka, K.; Tomita, A.; Setoyama, N.; Fukushima, Y.; Kyotani, T. *Chem. Mater.* **2005**, *17*, 5187.
23. Derradji, N. E.; Mahdjoubi, M. L.; Belkhir, H.; Mumumbila, N.; Angleraud, B.; Tessier, P. Y. *Thin Solid Films* **2005**, *482*, 258.
24. An, K. H.; Kim, W. S.; Park, Y. S.; Moon, J. M.; Bae, D. J.; Lim, S. C.; Lee, Y. S.; Lee, Y. H. *Adv. Funct. Mater.* **2001**, *11*, 387.
25. Raymundo-Pinero, E.; Leroux, F.; Beguin, F. *Adv. Mater.* **2006**, *18*, 1877.